



Impact of Pressure and Rotational Speed on the Efficiency of Dry Ice Blasting Machines: A Computational Fluid Dynamics Analysis

Azeef Khan Azlim Khan¹, Adi Azriff Basri^{1,*}, Mohd Zuhri Mohamed Yusoff², Azizan As'arry², Muhammad Shahril Shahbudin³, Ezzat Afifi Abd Halid³, Muhammad Safwan Abdul Aziz³

¹ Department of Aerospace Engineering, Faculty of Engineering, Universiti Putra Malaysia, 43400, Serdang, Selangor Darul Ehsan, Malaysia

² Department of Mechanical and Manufacturing Engineering, Faculty of Engineering, Universiti Putra Malaysia, 43400, Serdang, Selangor, Malaysia

³ AHS Solutions Sdn Bhd, No. 12, Jalan Tiara Sentral 1, Nilai Utama, Enterprise Park, 71800 Nilai, Negeri Sembilan, Malaysia

ARTICLE INFO

Article history:

Received 3 January 2025

Received in revised form 7 February 2025

Accepted 7 April 2025

Available online 30 April 2025

Keywords:

Dry ice machine; computational fluid dynamics; pressure change; rotational speed changes effect

ABSTRACT

Dry ice cleaning machines have become a highly effective solution in industrial cleaning, utilizing dry ice pellets to remove contaminants without damaging surfaces. This method, known as dry-ice blasting, uses compressed air to propel dry ice pellets, offering a cleaner alternative to traditional chemical and high-pressure water jet methods. The performance and effectiveness of dry ice cleaning machines are largely determined by the flow dynamics of the dry ice as it interacts with the cleaning surface. This study uses Computational Fluid Dynamics (CFD) to analyze the impact of operational parameters, specifically on rotational speed changes effect of gear and pressure inlet settings. The rotational speed are tested at 100, 250, and 500 rotational per minutes (rpm) to observe its effect on flow, while pressure variations of 8, 10, and 12 bar were examined to understand their influence on fluid behavior, ultimately enhancing machine efficiency and design. In conclusion, the analysis reveals that operating the dry ice machine at 250 rpm with an inlet pressure of 12 bar offers the best performance. This combination results for 12 bar shows 9.13% increment in exit velocity, reaching 1269 m/s compared to 1159 m/s at 10 bar. The nozzle pressure also increases by 17.66%, from 556.1 kPa to 654.3 kPa, ensuring stable flow dynamics. Additionally, the turbulent kinetic energy (TKE) rises by 19.62% to 43,770 m²/s², improving particle mixing and distribution. This optimal setting enhances machine efficiency and effectiveness, making it the ideal choice for dry ice spraying operation.

1. Introduction

In the realm of industrial cleaning, dry ice cleaning machines have emerged as an innovative and effective solution, utilizing the unique properties of dry ice pellets to remove contaminants without damaging the underlying surfaces. Dry-ice blasting, a pneumatic jet-based cleaning method using dry-ice pellets, is introduced as an alternative to traditional chemical and high-pressure water jet processes. Dry-ice pellets are produced from carbon dioxide, a natural resource, and have a hardness

* Corresponding author.

E-mail address: adiazriff@upm.edu.my

<https://doi.org/10.37934/ard.128.1.4763>

similar to gypsum. The process offers advantages such as no residue, minimal disposal costs, and shorter machining times. Dry-ice blasting is used in various industries, including nuclear, marine, aircraft, and train industries, for cleaning and decontamination purposes.

For example, in automotive industry, dry ice blasting machine has reduced the cost of collecting the cleaning media using the sublimation of dry ice particles [1]. Another study by Rajiv Kohli [2] shows that this machine decreased the probability of rust formation and protects electrical control wirings. In aerospace industry, mainly the usage of ice blasting machine is used for cleaning aircraft engines from contaminants in order to maintain the efficiency of gas turbine engines [3-5]. In energy industry, this machine also being use to clean the contaminants of oil, combustion deposits, harmful chemicals or others which cause fouling of blades function in gas turbine compressor [2,6].

Several studies had been conducted in improving the mechanism of dry ice machine in conjunction to produce optimize design of dry ice machine. G. Spur *et al.*, [7] studied the impact forces in dry-ice blasting were experimentally analyzed to understand the deformation and surface damage of the blasting material and the kinetic energy of the dry-ice pellets. The research contributes to existing knowledge by providing a detailed analysis of the dry-ice blasting mechanism, focusing on the impact forces, pellet diameter and velocity, and material removal process. The key findings include the thermo-mechanical effect of dry-ice blasting, with thermal contributing to 60% and kinetic to 40% of the process.

P. Kumar *et al.*, [8] discussed the impact of contamination on the insulation system of turbine generators and introduce Dry Ice Cleaning (DIC) as an effective and eco-friendly method for maintaining these systems. It introduces DIC as an effective method for cleaning windings and cores, presenting a case study on its application in a 120MW, 11KV turbine generator. The paper conducts comparative analysis by highlighting the advantages and disadvantages of DIC compared to traditional cleaning methods, such as reduced time and cost, elimination of secondary waste, and improved dielectric properties versus loud noise, the need for trained personnel, and ventilation for CO₂ gas release.

Masa *et al.*, [9] contributes to existing knowledge by presenting the innovation of replacing the pneumatic drive of a dry ice blasting machine with an electrical drive, leading to a significant reduction in compressed air consumption and corresponding electrical energy savings of 19%. The key findings include the measurement of shaving mechanism drive consumption, which accounts for approximately 19% of the total consumption, and the substitution of the pneumatic drive with an asynchronous three-phase electric motor and a frequency converter, resulting in a reduction of compressor electrical energy consumption from 7.5 kWh/h to 0.55 kWh/h.

Masa *et al.*, [10] contributes to existing knowledge by introducing energy-saving measures for dry ice blasting systems, focusing on minimizing compressed air consumption. The key findings include the identification of minimum compressed air flow rates and pressures for transporting dry ice pellets, replacing pneumatic drives with electric drives for energy savings, and controlling compressor performance and using electric motors with frequency converters to decrease electrical energy consumption. The study also introduces a new specific energy consumption measurement for dry ice blasting, which allows for comparison of energy consumption between different blasting systems. The experiments showed a potential 87% reduction in energy consumption with the implementation of these measures.

Phloymuk *et al.*, [11] The paper employs a methodology that assesses the condition of electrical rotating machine insulation using three characteristics: polarization and depolarization current, polarization index, and dielectric loss tangent. It compares the insulation characteristics of a 16.25 MVA synchronous generator before and after cleaning with dry ice blasting. The results show a decrease in polarization current, an increase in polarization index, and a lower loss tangent for the

clean winding, indicating improved insulation resistivity and reduced power loss. Dry ice blasting was found to be 300% faster than traditional solvent methods, leading to reduced maintenance downtime and increased productivity.

Hence, the efficiency and effectiveness of these machines are significantly influenced by the flow characteristics of the dry ice as it interacts with the cleaning surface. Therefore, understanding the fluid dynamics within the system is crucial for optimizing performance and ensuring reliable operation.

This study focuses on conducting a Computational Fluid Dynamics (CFD) analysis of the dry ice cleaning machine to investigate the effects of varying operational parameters. Specifically, the analysis examines the influence of rotational speed (RPM) and pressure settings on the system's performance. The RPM was varied at three distinct level of 100 RPM, 250 RPM, and 500 RPM in order to assess how changes in the speed of dry ice impact the flow dynamics. Additionally, pressure variations of 8 bar, 10 bar, and 12 bar were explored to further understand their effect on the system's fluid behavior. Ultimately, the results of this study will not only enhance the design and operational efficiency of dry ice cleaning machines but also contribute to the broader knowledge base in the field of industrial cleaning technologies.

2. Methodology

2.1 3D Model

In this study, the design of a 3D model of the Dry Ice Machine is prepared with the aid of the Computer-Aided Design (CAD) software called SolidWorks. The design is then further imported to the ANSYS WorkBench for the CFD Analysis (Figure 1).

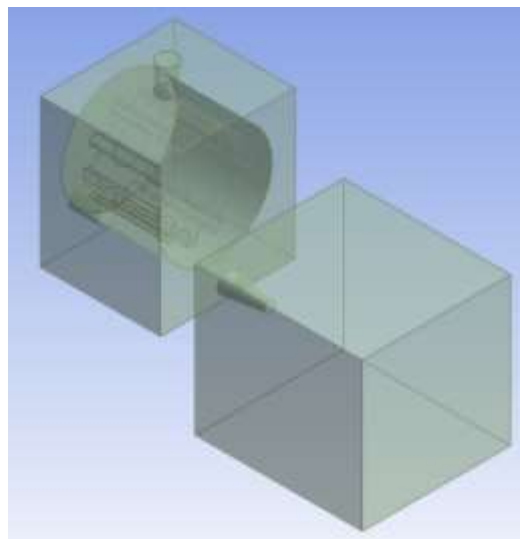


Fig. 1. 3D Model of dry ice machine using ANSYS design modeler

2.2 Computational Fluid Dynamics

CFD uses numerical methods such as discretization, solvers, and grid generation to simulate fluid systems. Solving these problems requires understanding the fluid's physical properties and applying mathematical equations, like the Navier-Stokes equations, which are based on conservation laws. The principle of conservational law is the change of properties, for example, mass, energy, and

momentum, subjected to input and output. For example, the change of mass in the object is as in Eq. (1) and (2) as follows [12-15] [1]:

$$\frac{dM}{dt} = \dot{m}_{in} - \dot{m}_{out} = 0 \quad (1)$$

$$\dot{m}_{in} = \dot{m}_{out} \quad (2)$$

Navier-Stokes equation is obtained by applying the mass (continuity equation), momentum (momentum equation) and boundary conditions in terms of relative velocities; $U_r=V_r; U_z=V_z; U_\theta=(V_\theta+\Omega r)$. Based on a few assumptions [2], the simplified conservations Eqs. (3) – (9) are as follows:

Continuity Equation:

$$\frac{\partial V_r}{\partial r} + \frac{V_r}{r} = 0 \quad (3)$$

θ -Momentum Equation:

$$V_r \frac{\partial V_\theta}{\partial r} + \frac{V_r V_\theta}{r} + 2\Omega V_r = \nu \frac{\partial^2 V_\theta}{\partial z^2} \quad (4)$$

r-Momentum Equation:

$$V_r \frac{\partial V_r}{\partial r} - \Omega^2 r - 2\Omega V_\theta - \frac{V_\theta^2}{r} = -\frac{1}{\rho} \frac{dp}{dr} + \nu \frac{\partial^2 V_r}{\partial z^2} \quad (5)$$

z-Momentum Equation:

$$\frac{\partial P}{\partial z} = 0 \quad (6)$$

Boundary Condition:

$$\text{at } r = r_2 \quad \bar{V}_r = \bar{V}_{r2} \quad \bar{V}_\theta = \bar{V}_{\theta2} \quad (7)$$

$$\text{at } z = 0, b \quad \bar{V}_r = 0 \quad \bar{V}_\theta = 0 \quad (8)$$

$$\text{at } z = \frac{b}{2} \quad \frac{\partial V_r}{\partial z} = \frac{\partial V_\theta}{\partial z} = 0 \quad (9)$$

2.3 Mesh Discretization

The mesh for the dry ice machine consists of 309,536 elements, using an element size of 5 mm (Figure 2). The mesh quality was assessed by evaluating the skewness, which is a critical parameter for determining mesh accuracy and solution stability. The maximum skewness obtained is 0.7982, indicating that the mesh is of good quality, as it falls within the acceptable range. The selected mesh will be employed for subsequent analyses under different operational conditions, ensuring consistency in the simulation framework as the inlet pressure and rotational speeds are varied.



Fig. 2. Mesh of the 3D model

The optimum mesh for the dry ice machine was determined through a mesh dependency test. This test ensures that the simulation results are not significantly influenced by further mesh refinement, providing a balance between accuracy and computational efficiency. The results showed that the maximum pressure at the outlet became constant as the mesh reached approximately 300,000 elements. Beyond this point, additional refinement did not result in significant changes in pressure values, confirming that the solution had stabilized (Figure 3).

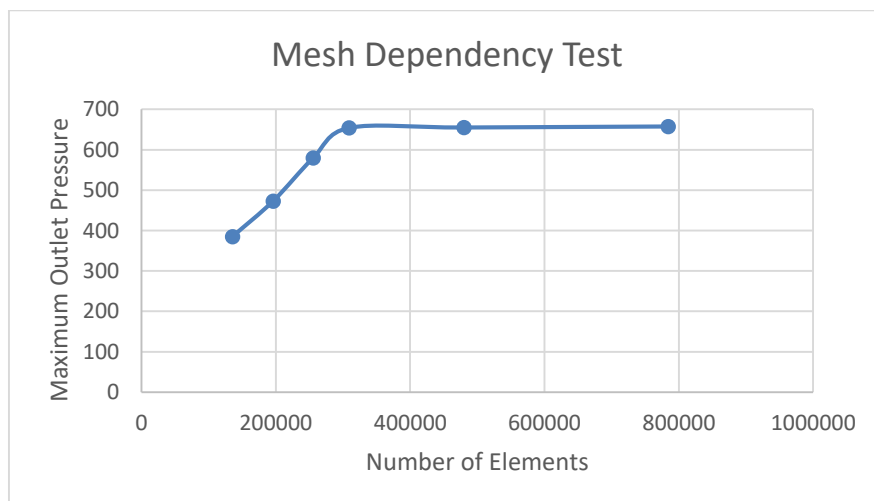


Fig. 3. Mesh dependency test

2.4 Boundary Condition

The boundary consists of flow of inlet 1 and 2, the outlet and the wall. The boundary conditions are shown in the Figure 4 and in the Table 1.

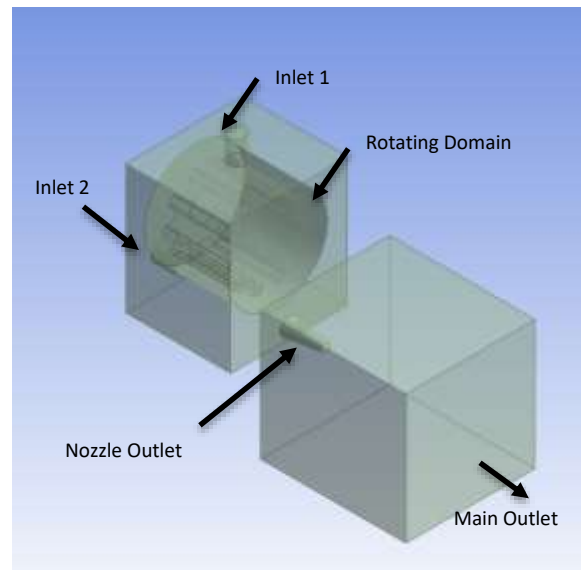


Fig. 4. Boundary condition domain

Table 1 displays the boundary conditions used to run the simulation. These boundary conditions ensure the simulation is realistic and stable, reflecting the actual operation of the dry ice machine. Properly defined inlet and outlet conditions help in achieving accurate flow rates and pressures, while the wall and rotational conditions ensure the correct interaction between the machine components and the fluid.

Table 1

Boundary conditions

Boundary conditions	Values
Pressure Outlet	0 Pa
Domain 1	Air
Domain 2	Moving Mesh With Rotating Region (X-Axis)
Rotation per minutes (rpm)	100,250 & 500
Viscous Model	k-epsilon
Inlet 1	2 m/s
Inlet 2	8 Bar, 10 Bar & 12 Bar
Residual Error	10^{-6}

3. Results

3.1 Pressure Effect at 100 rpm Speed

3.1.1 Pressure distribution

Table 2 (a) presents the pressure distribution of the dry ice machine operating at 100 RPM, measured at different inlet pressures of 8 bar, 10 bar, and 12 bar. The results indicate that the pressure in the gear domain is consistently higher, with a gradual reduction observed towards the nozzle outlet across all inlet pressures. At the nozzle outlet, the highest-pressure magnitude is achieved with a 12-bar inlet, reaching 683.1 kPa, followed by 566.4 kPa at 10 bar, and 454 kPa at 8 bar (Figure 5). Further details are illustrated by the pressure distribution along the pathline from Inlet 2 to the nozzle outlet, as shown in Table 2(b). The graph reveals a typical pressure distribution pattern: starting with an initial pressure of at the inlet, followed by a gradual reduction along the

pathline, and a significant pressure drop near the nozzle outlet for each inlet pressure. Among the tested inlet pressures, the highest pressure along the pathline is observed at 12 bar with 520 kPa, followed by 10 bar with 440 kPa, and 8 bar with 370 kPa. This behavior highlights the correlation between inlet pressure and pressure drop across the nozzle.

Table 2

The pressure contour and pathline pressure graph for different pressure inlet at 100 rpm

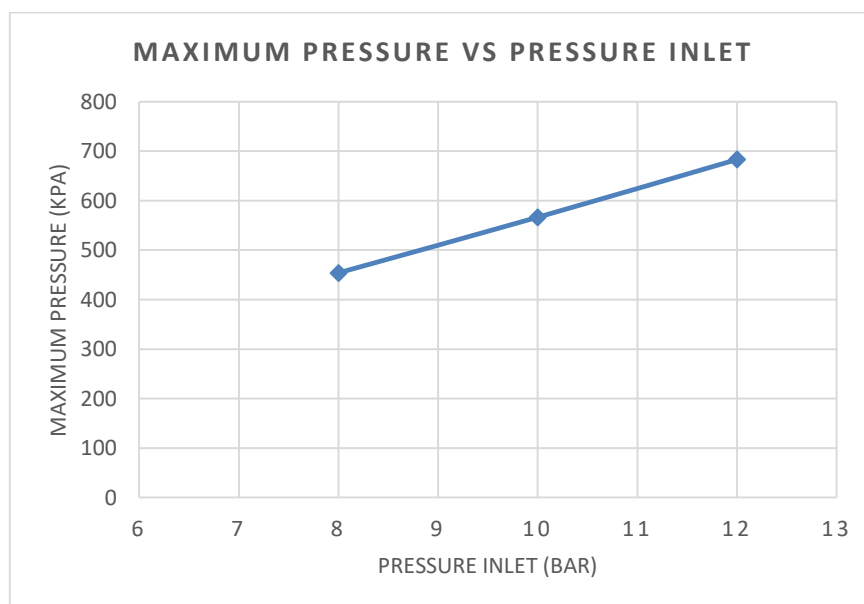
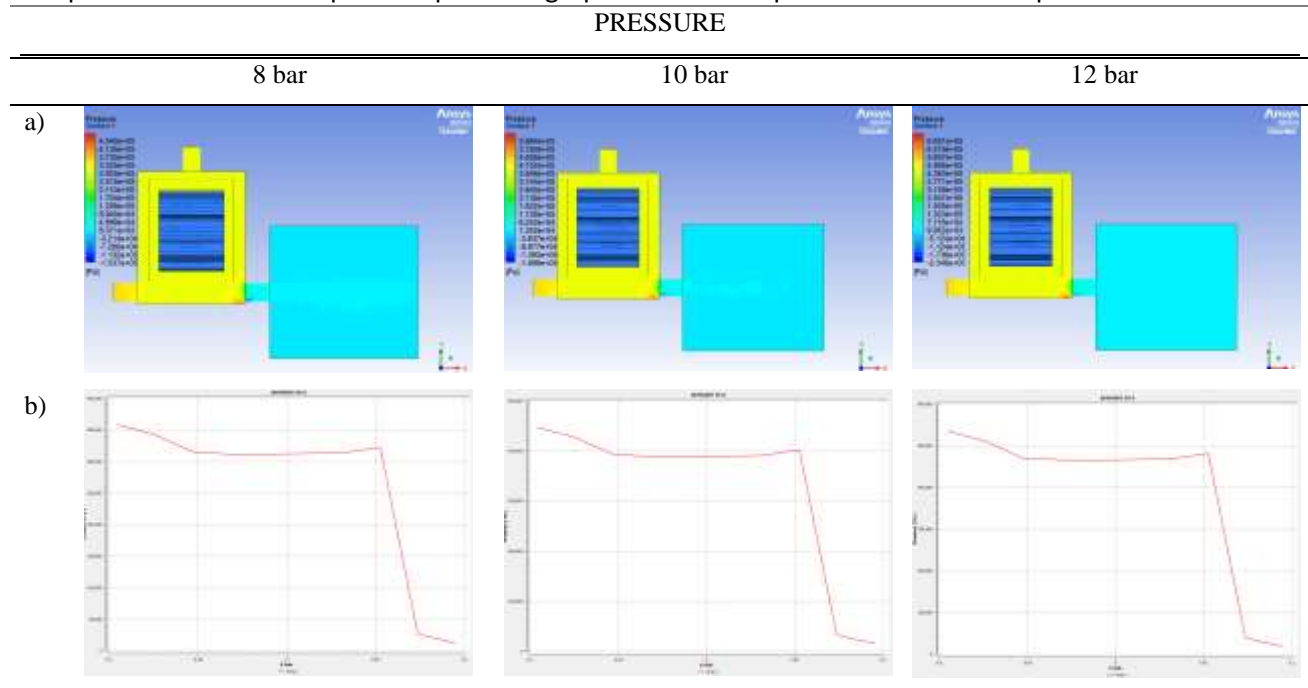


Fig. 5. Maximum pressure effect on different pressure inlet at 100 rpm

3.1.2 Velocity distribution

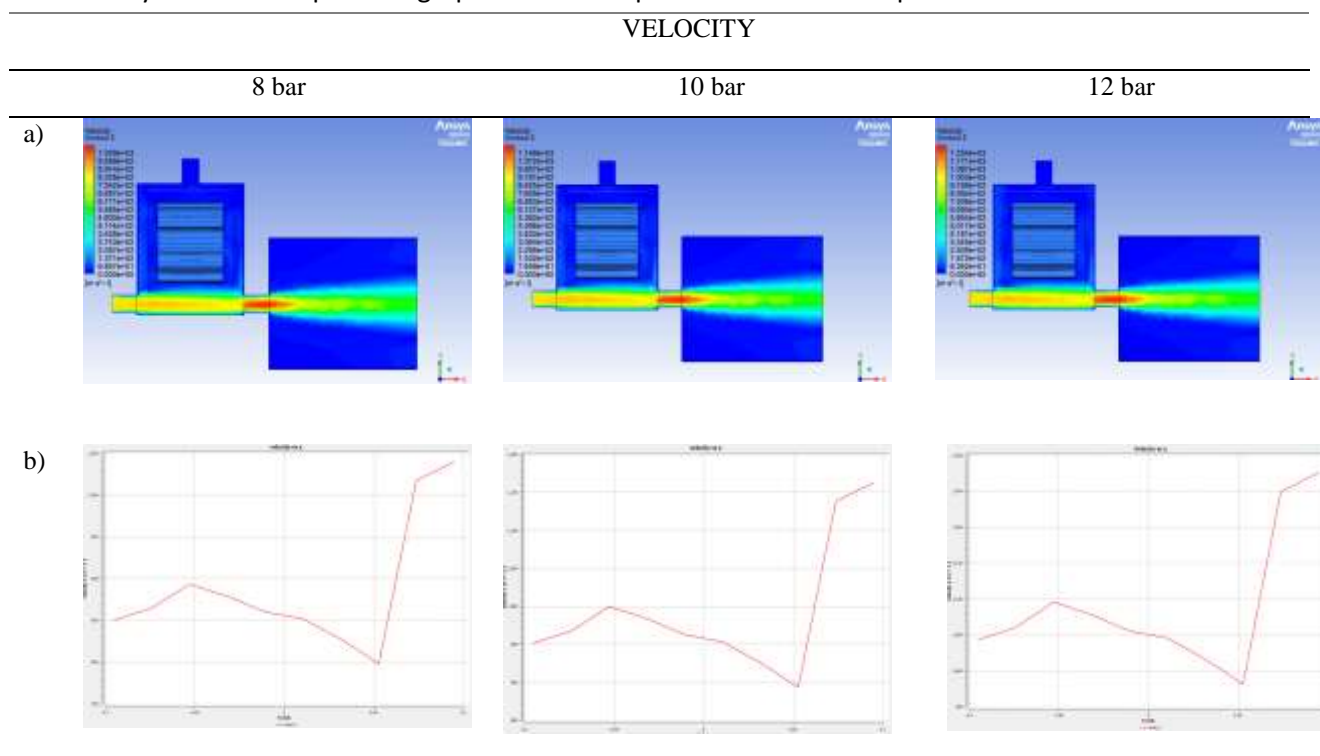
Table 3 (a) presents the velocity contours of the dry ice machine operating at 100 RPM under varying inlet pressures of 8 bar, 10 bar, and 12 bar. It is observed that the maximum velocity occurs

at the outlet exit for each case, with higher inlet pressures generating higher outlet velocities. At the nozzle exit, the maximum velocity for 12 bar is 1254 m/s, followed by 10 bar at 1149 m/s, and 8 bar at 1029 m/s (refer Figure 6). This demonstrates a direct correlation between inlet pressure and flow velocity as the inlet pressure increases, the velocity at the outlet rises accordingly. High exit velocities are essential for efficient performance in dry ice spraying applications, as they increase the impact force and enhance operational effectiveness. Further insights into the velocity distribution are provided along the pathline from Inlet 2 to the nozzle outlet as shown in Table 3 (b). At the inlet, the initial velocity starts at 850 m/s for 8 bar, 950 m/s for 10 bar, and 1040 m/s for 12 bar. As the flow progresses, the velocity increases slightly due to flow acceleration within the system.

A minor peak in velocity is observed midway along the pathline, likely caused by flow constriction or localized pressure changes. Following this peak, a slight reduction in velocity occurs due to energy losses along the flow path. However, as the flow approaches the nozzle outlet, a sharp acceleration takes place, with the maximum velocities recorded at the exit for each inlet pressure. This pattern indicates that higher inlet pressures not only result in greater initial velocities but also achieve higher outlet velocities, thereby enhancing the performance of the dry ice machine. These findings highlight the importance of selecting the appropriate inlet pressure to optimize the machine's efficiency based on operational requirements.

Table 3

The velocity contour and pathline graph at different pressure inlet at 100 rpm



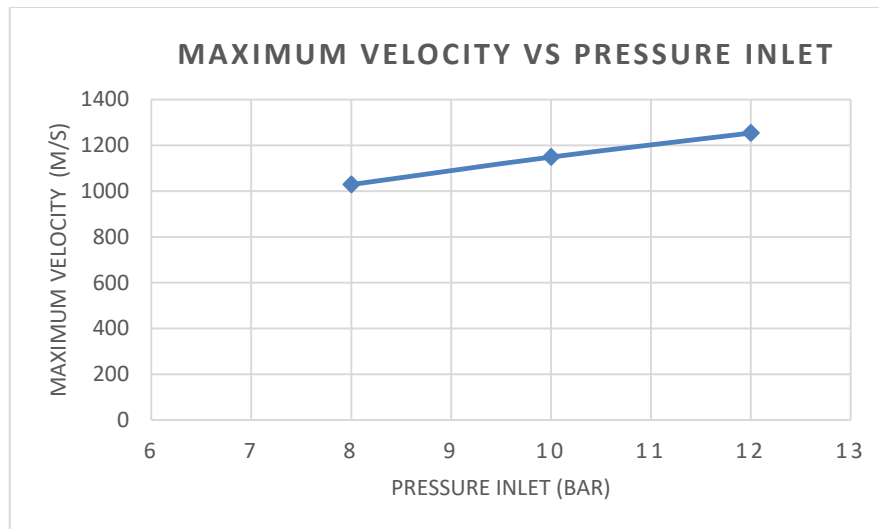


Fig. 6. Maximum velocity effect on different pressure inlet at 100 rpm

3.1.3 Turbulence kinetic energy distribution

Table 4 (a) presents the turbulence kinetic energy (TKE) values of the dry ice machine operating at 100 RPM for inlet pressures of 8 bar, 10 bar, and 12 bar. The TKE values indicate the amount of turbulent energy present in the flow, which plays a critical role in determining the efficiency of particle mixing and spraying. At an inlet pressure of 12 bar, the TKE reaches its highest value of 47,050 m^2/s^2 , reflecting the strong turbulent fluctuations within the flow. As the inlet pressure decreases, the TKE reduces to 39,330 m^2/s^2 at 10 bar and further to 33,340 m^2/s^2 at 8 bar. This trend highlights the direct relationship between inlet pressure and turbulence, where higher inlet pressures lead to stronger turbulence. The elevated TKE at 12 bar suggests that the flow contains more energy within its turbulent eddies and vortices, potentially enhancing the dry ice spraying process by improving particle dispersion and impact force. In contrast, the lower TKE values at 10 bar and 8 bar indicate less turbulent energy, which may result in reduced particle mixing and lower spraying efficiency.

Figure 7 illustrates the TKE distribution along the pathline for the dry ice machine operating at 250 RPM with inlet pressures of 8 bar, 10 bar, and 12 bar. The initial TKE values at Inlet 2 highlight how turbulent energy builds up within the system as the flow progresses. At Inlet 2, the initial TKE is 3,000 m^2/s^2 for 8 bar, 3,800 m^2/s^2 for 10 bar, and 4,000 m^2/s^2 for 12 bar. As the flow moves through the system, the TKE increases due to interactions within the flow, such as shear effects, pressure changes, and turbulence development. The trend shown in the graph suggests that higher inlet pressures correspond to greater turbulence throughout the flow path. The increase in TKE along the pathline demonstrates the influence of pressure on generating more turbulent energy, which plays a key role in enhancing the efficiency of dry ice spraying. As observed, 12 bar maintains the highest TKE throughout the pathline, followed by 10 bar and then 8 bar.

The final peak in the TKE at the nozzle outlet highlights the impact of flow constriction, where turbulence intensifies just before the spray exits the system. This trend supports the conclusion that higher inlet pressures not only generate more initial turbulent energy but also sustain turbulence through the flow path, resulting in improved particle dispersion and impact performance.

Table 4

Turbulence kinetic energy contour and pathline graph at different pressure inlet at 100 rpm

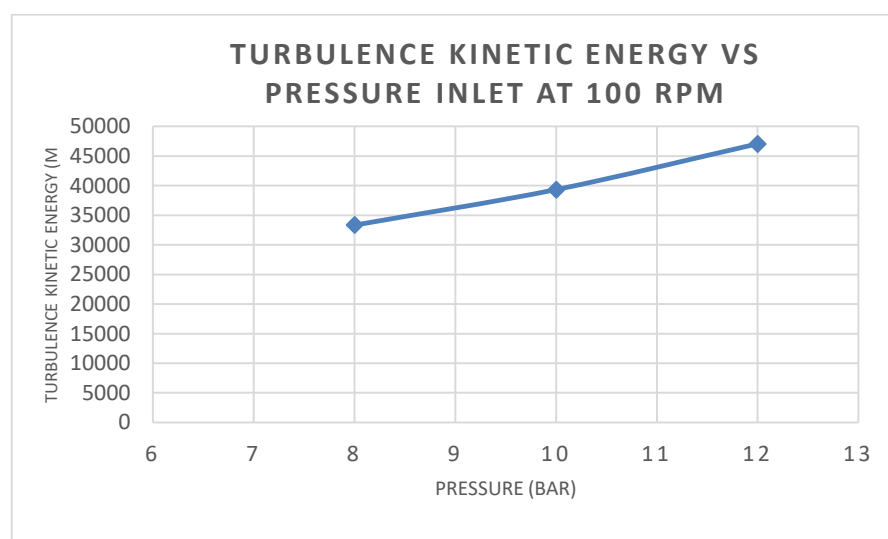
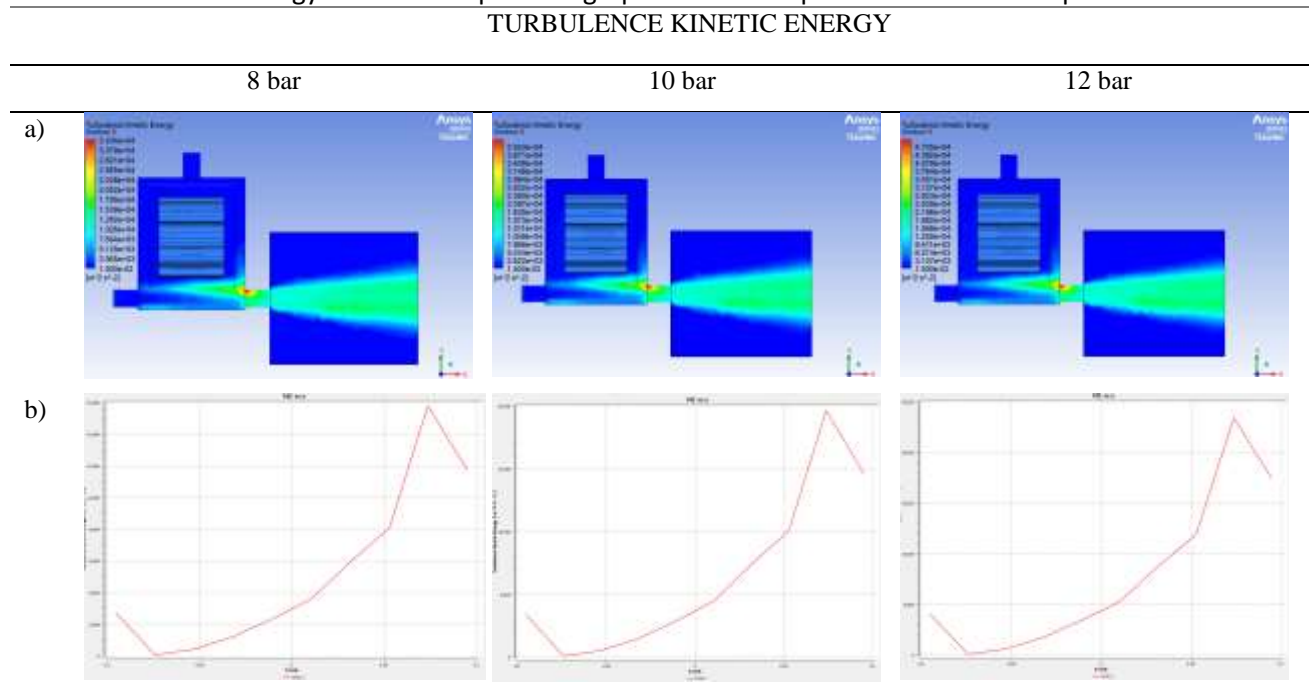


Fig. 7. Maximum turbulence kinetic energy on different pressure inlet at 100 rpm

3.2 Rotational Speed Changes Effect

3.2.1 Pressure distribution

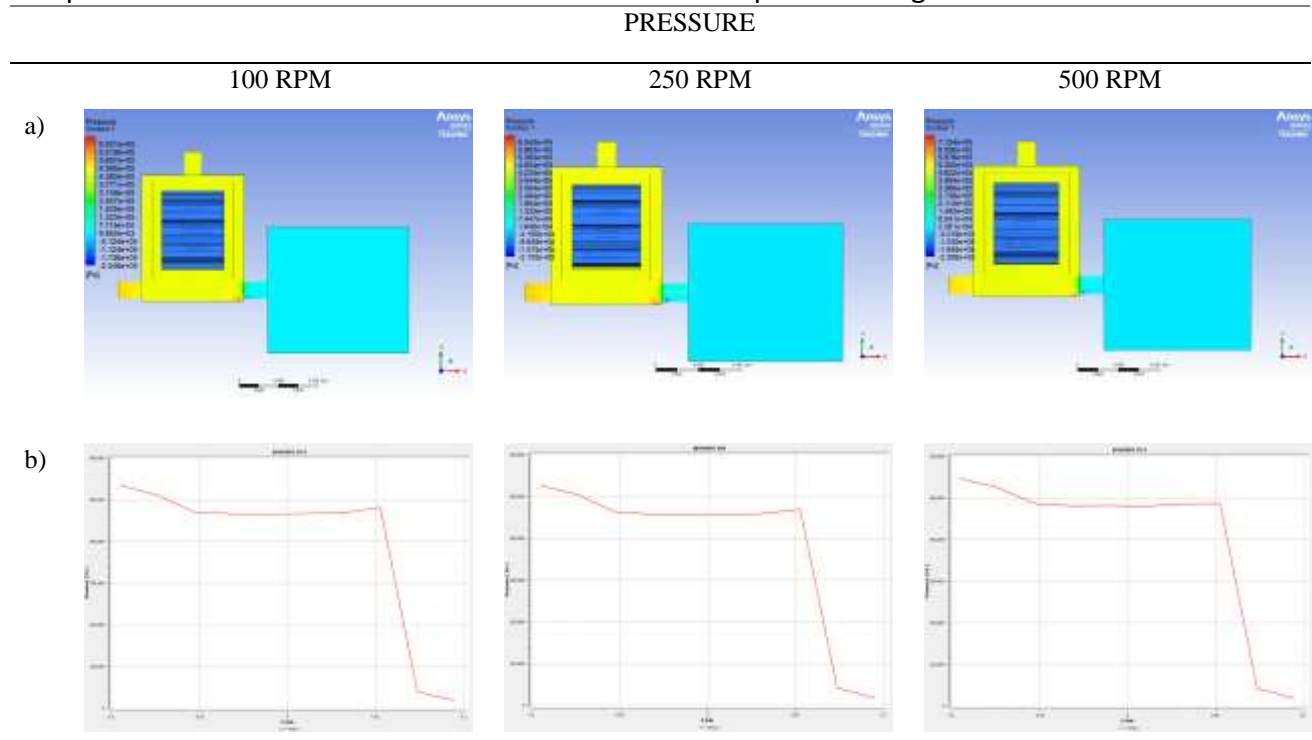
Table 5 (a) presents the pressure contour and its results of the dry ice machine operating at three different rotational speeds: 100 RPM, 250 RPM, and 500 RPM where the inlet pressure is 12 bar. The data demonstrates a clear correlation between RPM and pressure, with higher rotational speeds leading to greater system pressures. At 100 RPM, the pressure is recorded at 683 kPa, while at 250 RPM, the pressure shows a slight decrease to 654 kPa. The highest pressure is observed at 500 RPM, reaching 713 kPa. This trend reflects the machine's ability to generate higher pressures as the rotational speed increases. The increased pressure is essential for improving the system's performance, as higher pressures typically result in better fluid acceleration and impact force.

Table 5 (b) shows the pathline pressure distribution for the dry ice machine at the three tested RPM levels. The pathline pressure follows a consistent pattern, showing minor variations as the fluid moves through the system, influenced by energy losses along the flow path. At 100 RPM, the pathline pressure starts at 540 kPa, providing a moderate pressure level at this speed. For 250 RPM, the pathline pressure slightly decreases to 535 kPa, indicating a small drop compared to the lower RPM. At 500 RPM, the pathline pressure increases again to 545 kPa, illustrating the system's capacity to sustain higher pressures at greater rotational speeds.

As observed in the pressure results, higher RPMs contribute to maintaining stable and elevated pressures along the pathline, ensuring optimal performance of the system, especially in dry ice spraying processes that rely on maintaining high pressures for effective operation.

Table 5

The pressure contour at 12 bar with different rotational speed of the gear



3.2.2 Velocity distribution

Table 6 (a) presents the maximum velocity results of the dry ice machine, derived from the velocity contour at three different rotational speeds: 100 RPM, 250 RPM, and 500 RPM. The data shows that the maximum velocity occurs at the outlet exit, with different RPMs yielding similar high velocities, essential for efficient dry ice spraying.

At 100 RPM, the maximum velocity is recorded at 1254 m/s, while at 250 RPM, the velocity increases slightly to 1269 m/s. At 500 RPM, the velocity slightly decreases to 1259 m/s. This trend reflects the machine's ability to maintain high outlet velocities across varying rotational speeds, with a slight increase at 250 RPM. Higher velocities are crucial for achieving better spray dispersion and impact force, which are critical for the dry ice spraying process.

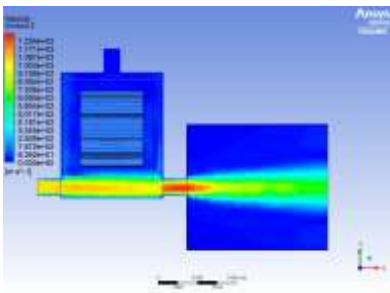
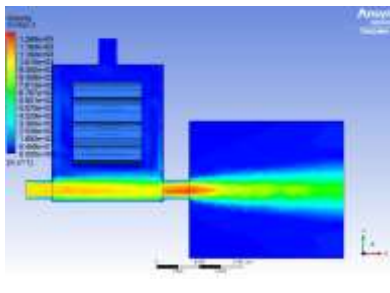
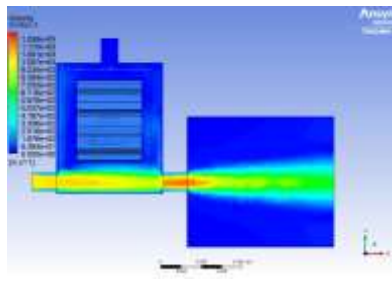
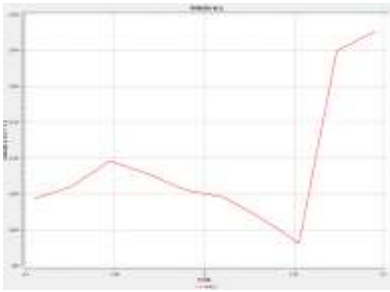
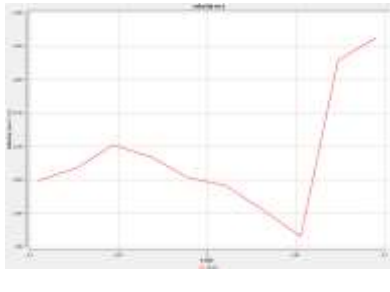
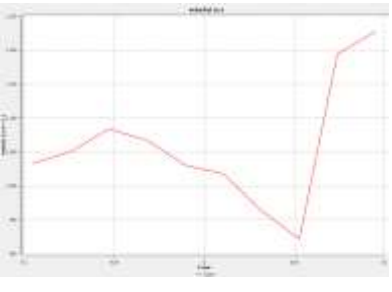
Table 6 (b) presents the initial velocity distribution along the pathline for the dry ice machine, showing the velocity as the fluid moves from the inlet to the outlet nozzle at the three different RPM levels. The pathline velocity shows a slight variation across RPMs, with a gradual increase in velocity

as the system accelerates the fluid. The velocity distribution along the pathline follows a characteristic trend, as shown in the attached graph based on Table 6 (b). Initially, the velocity starts at a moderate level and steadily increases as the fluid moves through the system. After reaching a peak, the velocity experiences a slight decline, indicating potential energy losses or deceleration along the flow path. However, near the nozzle outlet, the velocity increases sharply, representing the fluid's final acceleration as it exits the system. This sharp rise is crucial, as it ensures high outlet velocities, essential for maximizing the impact force in dry ice spraying applications.

At 100 RPM, the initial velocity is 1040 m/s, rising to a maximum velocity of 1254 m/s. For 250 RPM, the initial velocity increases slightly to 1050 m/s, with a maximum velocity of 1269 m/s. Finally, at 500 RPM, the initial velocity starts at 1030 m/s, culminating in a maximum velocity of 1259 m/s. This data aligns with the trend observed, where velocities increase along the pathline, culminating in sharp rises near the outlet for optimal system performance.

Table 6

Velocity contour at 12 bar with different rotational speed of the gear

VELOCITY			
	100 RPM	250 RPM	500 RPM
a)			
b)			

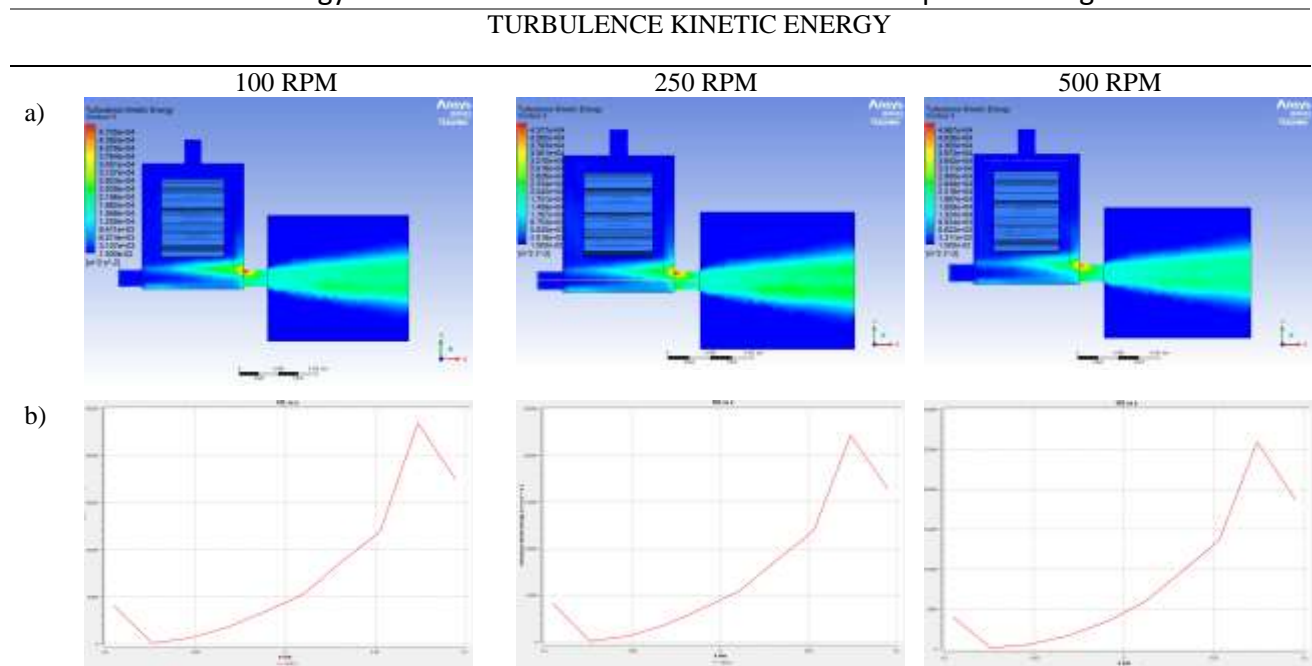
3.2.3 Turbulence kinetic energy distribution

The analysis of Turbulent Kinetic Energy (TKE) at different RPMs reveals notable variations in maximum TKE values. Based on Table 7 (a), at 100 RPM, the maximum TKE is recorded at 47,050, demonstrating a significant level of turbulence. However, as the RPM increases to 250, the maximum TKE slightly decreases to 43,770. This drop may indicate a temporary disruption in flow dynamics at this rotational speed. Interestingly, at 500 RPM, the maximum TKE reaches its highest point at 49,670, suggesting that increased rotational speed enhances turbulence significantly. This trend emphasizes the positive correlation between RPM and turbulence intensity, which is critical for improving the dispersion and efficiency of the dry ice spray system.

The initial TKE analysis along the pathline at Inlet 2 to the outlet as shown in Table 7 (b) presents a relatively stable pattern across different RPMs. At both 100 and 250 RPM, the initial TKE values are consistently recorded at 4000, indicating a uniform level of turbulence at the onset of the flow. However, at 500 RPM, there is a slight decrease in initial TKE to 3800. This reduction may suggest a transitional phase in the flow dynamics as the system ramps up speed. Overall, the stable initial TKE values highlight that, despite variations in RPM, the turbulence levels at the inlet remain fairly consistent before increasing towards the outlet, setting the stage for the subsequent rise in maximum TKE as the fluid accelerates through the system.

Table 7

Turbulence kinetic energy contour at 12 bar with different rotational speed of the gear









3.3 Roughness Surface Test

Table 8 and Figure 8 present the surface roughness test data of the flat plate before and after applying dry ice blasting. Specimen 7 represents the surface area of the flat plate before dry ice blasting, while Specimen 8 represents the surface area after the treatment (Table 7). Figure 8 shows a significant improvement in surface roughness across all measured locations (A, B, and C). At Location A, the surface roughness before the dry ice blasting was $6.421 \mu\text{m}$, which improved to $0.801 \mu\text{m}$ after the treatment, indicating an 87.53% improvement. At Location B, the roughness value decreased from $6.801 \mu\text{m}$ to $0.893 \mu\text{m}$, reflecting an 86.87% improvement. Similarly, at Location C, the roughness value dropped from $1.827 \mu\text{m}$ to $0.726 \mu\text{m}$, showing a 60.26% improvement. These results highlight the effectiveness of dry ice blasting in significantly enhancing surface roughness.

Table 8

Image of roughness surface test before and after dry ice blast

Condition/ Location	A	B	C
Before			
After			

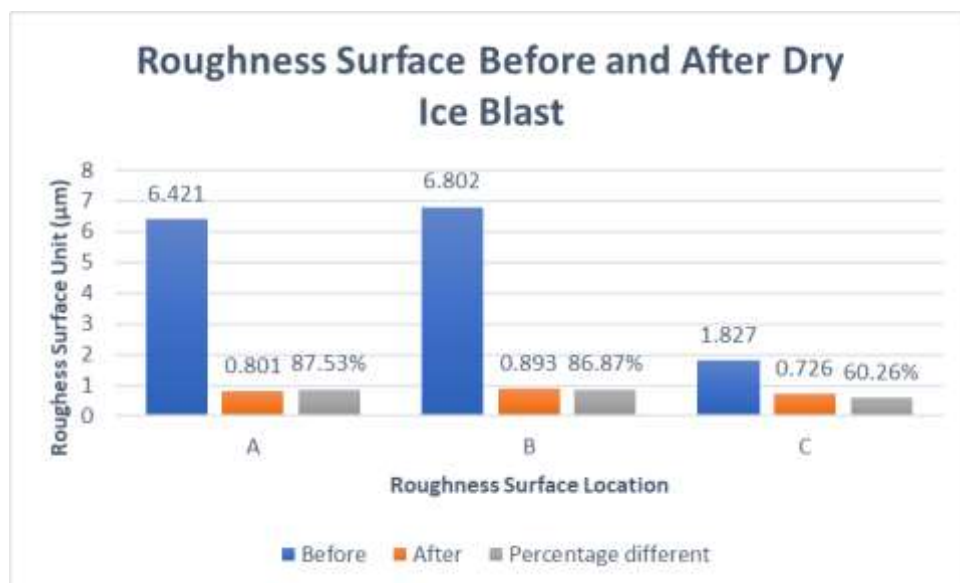


Fig. 8. Roughness surface test before and after dry ice blast

4. Discussion

4.1 Pressure Effects at 100 rpm Speed

The analysis confirms that 12 bar is the optimal inlet pressure, achieving the highest performance across multiple metrics. At the nozzle outlet, 12 bar produces 683.1 kPa, which is 20.6% higher than the 566.4 kPa at 10 bar and 50.5% higher than the 454 kPa at 8 bar. This enhanced pressure stability minimizes fluctuations and energy losses, ensuring consistent flow and reliable dry ice spraying. In terms of velocity, the 12-bar setup yields a peak exit velocity of 1254 m/s, which is 9.1% greater than the 1149 m/s at 10 bar and 21.9% higher than the 1029 m/s at 8 bar. The increased velocity results in stronger impact force and wider spray coverage, crucial for effective applications. The smooth acceleration along the flow path highlights improved energy transfer and efficiency at the higher inlet pressure.

Additionally, 12 bar produces a turbulence kinetic energy (TKE) of $47,050 \text{ m}^2/\text{s}^2$, marking an 19.6% increase over the $39,330 \text{ m}^2/\text{s}^2$ at 10 bar and 41.1% higher than the $33,340 \text{ m}^2/\text{s}^2$ at 8 bar. This heightened turbulence promotes better particle mixing and dispersion, leading to more effective spray patterns. With superior performance in pressure, velocity, and turbulence, 12 bar is the most effective choice for the next stage of analysis, which will focus on determining the ideal gear rotational speed using an inlet pressure of 12 bar.

4.2 Rotational Speed Changes Effect

Based on the comprehensive analysis of the dry ice machine's performance at various rotational speeds, it is concluded that 250 RPM emerges as the most suitable operating speed. At this RPM, the machine maintains a balanced performance characterized by optimal pressure, velocity, and turbulent kinetic energy (TKE). Specifically, the pressure is recorded at 654 kPa, which, while slightly lower than the pressures observed at 100 RPM (683 kPa) and 500 RPM (713 kPa), reflects a commendable stability without the energy inefficiencies associated with higher RPMs. In terms of maximum velocity, the 250 RPM setting yields a peak velocity of 1269 m/s, slightly surpassing the 100 RPM performance (1254 m/s) while being on par with the 500 RPM velocity of 1259 m/s. This illustrates that 250 RPM can achieve nearly the same level of efficiency in terms of fluid acceleration while avoiding the substantial power consumption associated with 500 RPM.

Additionally, the turbulent kinetic energy analysis reveals a peak TKE of 43,770 at 250 RPM, striking an optimal balance in turbulence intensity necessary for effective dry ice dispersion, without the transient drop in performance noted at higher RPMs.

Choosing 500 RPM is not recommended, as it results in the highest energy consumption without significant improvements in performance metrics, reflecting the diminishing returns of increased RPM. In summary, 250 RPM stands out as the optimal choice, providing an effective balance of performance and energy efficiency, ensuring reliable and consistent operation of the dry ice machine while maximizing spraying effectiveness.

4.3 Roughness Surface Test Effect

Based on the previous results of roughness surface test, it can be concluded that the implementation of dry ice blast had improved the surface quality of the flat plate. The roughness surface value reduce around 87.53%, 86.87% and 60.26% for the respective location of A, B and C. The high pressure flow from the dry ice blast had showed and effective in cleaning the flat plate surface

from the rust and produced a smoother surface compared with the surface without implementing the dry ice blast machine.

4. Conclusions

In conclusion, the analysis demonstrates that 250 RPM coupled with an inlet pressure of 12 bar represents the optimal operating conditions for the dry ice machine. This combination significantly enhances the machine's performance metrics across multiple dimensions. At 250 RPM, the maximum exit velocity is recorded at 1269 m/s, which is a 9.13% increase compared to the 1159 m/s observed at 10 bar, underscoring the efficiency in dry ice spraying applications. Moreover, the pressure at the nozzle outlet reaches 654.3 kPa under the 12 bar setting, reflecting a 17.66% increase from the 556.1 kPa observed at lower pressures. This elevation in outlet pressure ensures consistent flow dynamics, reducing the risk of fluctuations during operation. Additionally, the turbulent kinetic energy (TKE) at 12 bar is measured at 43,770 m²/s², a 19.62% increase over the 36,440 m²/s² at 10 bar. This higher TKE facilitates improved mixing and distribution of dry ice particles, crucial for achieving effective spraying outcomes. Thus, the synergy between 250 RPM and 12 bar establishes a reliable and efficient operational framework, optimizing the machine's capabilities for superior performance in dry ice spraying applications. In addition, the study also proved that the implementation of dry ice blast had improved the smoothness of the surface with average of 78.22% of improvement compare with the flat plat surface without implementing the dry ice blast. This strategic combination not only maximizes operational efficiency but also enhances the overall effectiveness of the spraying process, confirming its status as the best choice for the dry ice machine's operational parameters.

Acknowledgement

The authors would like to thank the Faculty of Engineering, Universiti Putra Malaysia and AIIS Solutions Sdn Bhd for all the support throughout this research study.

References

- [1] Baluch, Nazim, Shahimi Mohtar, and Che Sobry Abdullah. "Dry-ice blasting of auto robotic assemblies." *International Journal of Supply Chain Management* 5, no. 4 (2016): 97-103.
- [2] Kohli, Rajiv. "Applications of solid carbon dioxide (dry ice) pellet blasting for removal of surface contaminants." In *Developments in surface contamination and cleaning: applications of cleaning techniques*, pp. 117-169. Elsevier, 2019. <https://doi.org/10.1016/B978-0-12-815577-6.00004-9>
- [3] Chandrasekar, M. "A short review on alternative cleaning methods to remove scale and oxide from the jet engine alloys." *International Journal of Engineering Research and Technology* 4, no. 12 (2015).
- [4] Rudek, Arthur, David Muckenaupt, Rudolf Kombeitz, Thomas Zitzmann, Gerald Russ, and Barry Duignan. "Experimental and numerical investigation of CO₂ dry-ice based aircraft compressor cleaning." In *13 th European Conference on Turbomachinery Fluid dynamics & Thermodynamics*. EUROPEAN TURBOMACHINERY SOCIETY, 2019.
- [5] Dong, Shujuan, Bo Song, Bernard Hansz, Hanlin Liao, and Christian Coddet. "Improvement in the microstructure and property of plasma sprayed metallic, alloy and ceramic coatings by pre-/during-treatment of dry-ice blasting." *Surface and Coatings Technology* 220 (2013): 199-203. <https://doi.org/10.1016/j.surfcoat.2012.03.071>
- [6] R. E. Hefner and U. S. P. Documents, "(12) United States Patent," vol. 2, no. 12, 2016.
- [7] Spur, G., E. Uhlmann, and F. Elbing. "Dry-ice blasting for cleaning: process, optimization and application." *Wear* 233 (1999): 402-411. [https://doi.org/10.1016/S0043-1648\(99\)00204-5](https://doi.org/10.1016/S0043-1648(99)00204-5)
- [8] Kumar, P. G. S. "Dry ice cleaning to improvise dielectric features of high voltage windings in turbine generators." In *2013 IEEE 1st International Conference on Condition Assessment Techniques in Electrical Systems (CATCON)*, pp. 23-28. IEEE, 2013. <https://doi.org/10.1109/CATCON.2013.6737468>
- [9] Máša, Vítězslav, Pavel Kuba, Dalimil Petrilák, and Jakub Lokaj. "Decrease in consumption of compressed air in dry ice blasting machine." *Chem Eng* 39 (2014): 805-10. <https://doi.org/10.3303/CET1439135>

- [10] Máša, Vítězslav, and Pavel Kuba. "Efficient use of compressed air for dry ice blasting." *Journal of Cleaner Production* 111 (2016): 76-84. <https://doi.10.1016/j.jclepro.2015.07.053>
- [11] Phloymuk, Natthawut, and Nutthaphong Tanthanuch. "Improvement of Insulation for Rotating Machine by Dry Ice Method." *Procedia Computer Science* 86 (2016): 345-348. <https://doi.10.1016/j.procs.2016.05.093>
- [12] Faris, Ahmad Fariduddin Ahmad, Adi Azriff Basri, Ernie Illyani Basri, Ezanee Gires, Mohammed Thariq Hameed Sultan, and Kamarul Arifin Ahmad. "Propeller design and performance evaluation by using computational fluid dynamics (CFD): a review." *Journal of Aeronautics, Astronautics and Aviation* 53, no. 2 (2021): 263-274. [https://doi.10.6125/JoAAA.202106_53\(2\).19](https://doi.10.6125/JoAAA.202106_53(2).19)
- [13] Kamal, Nur Nabillah Mohd, Adi Azriff Basri, Ernie Illyani Basri, Mohammed Thariq Bin Haji Hameed Sultan, Azmin Shakrine Mohd Rafie, and Mohd Faisal Abdul Hamid. "Validation and verification of aerodynamics loading of Schrenk approximation, Prandtl lifting-line and computational fluid dynamics with experiment on NACA series." *Journal of Aeronautics, Astronautics and Aviation* 53, no. 2 (2021): 283-288.
- [14] Faris, Ahmad Fariduddin Ahmad, Adi Azriff Basri, Ernie Illyani Basri, Mohammed Thariq Hameed Sultan, and Kamarul Arifin Ahmad. "Aerodynamics effects of APC slow flyer propeller blade design with different airfoil origin positions." *Journal of Aeronautics, Astronautics and Aviation* 54, no. 3 (2022): 325-334. [https://doi.10.6125/JoAAA.202209_54\(3\).09](https://doi.10.6125/JoAAA.202209_54(3).09)
- [15] Nazri, Muhammad Nor Ikmal Muhamad, Nurul Qistina Mohamad Fadhir, Farid Bajuri, Ernie Illyani Basri, and Adi Azriff Basri. "Experimental Study of Improved Tesla Micro-Turbine." *Journal of Aeronautics, Astronautics and Aviation* 56, no. 1S (2024): 461-468.